Published in final edited form as:

Lab Invest. 2016 March ; 96(3): 270–282. doi:10.1038/labinvest.2015.147.

Lymphatic endothelial lineage assemblage during corneal lymphangiogenesis

Alicia L. Connor, **Philip M. Kelley**, and **Richard M. Tempero**

Boys Town National Research Hospital, Department of Neurosensory Genetics and Otolaryngology and Head and Neck Surgery, 555 North 30th Street, Omaha NE 68131

Abstract

Post natal inflammatory lymphangiogenesis presumably requires precise regulatory processes to properly assemble proliferating lymphatic endothelial cells (LECs). The specific mechanisms that regulate the assembly of LECs during new lymphatic vessel synthesis are unclear. Dynamic endothelial shuffling and rearrangement has been proposed as a mechanism of blood vessel growth. We developed genetic lineage tracing strategies using an inductive transgenic technology to track the fate of entire tandem dimer tomato positive (tdT) lymphatic vessels or small, in some cases clonal, populations of LECs. We coupled this platform with a suture induced mouse model of corneal lymphangiogenesis and used different analytic microscopy techniques including serial live imaging to study the spatial properties of proliferating tdT^+ LEC progenies. LEC precursors and their progeny expanded from the corneal limbal lymphatic vessel and were assembled contiguously to comprise a subunit within a new lymphatic vessel. VE-cadherin blockade induced morphologic abnormalities in newly synthesized lymphatic vessels, but did not disrupt the tdT^+ lymphatic endothelial lineage assembly. Analysis of this static and dynamic data based largely on direct *in vivo* observations supports a model of lymphatic endothelial lineage assemblage during corneal inflammatory lymphangiogenesis.

Introduction

The lymphatic vasculature is a network of vessels comprised of capillaries and larger collecting vessels that transport extracellular fluid and cells directly to regional lymph nodes, major centers of immunologic activity, and ultimately into the venous circulation. The physiologic functions of this system are essential for life (Alitalo, 2011). In the adult, the lymphatic vasculature regulates mechanisms of inflammation, immunity, and facilitates tissue repair following pathologic events. Disease conditions such as inflammation stimulate a remarkably plastic and in some cases irreversible process of new lymphatic vessel growth (Karpanen and Alitalo, 2008;Wuest and Carr, 2010;Yao et al, 2010). Lymphangiogenesis requires the coordination of proliferating lymphatic endothelial cells (LECs), regulated by many factors, most notably vascular endothelial growth factor C (VEGF-C) (Tammela and

Corresponding author: Richard M. Tempero, 555 North 30th Street, Omaha, NE 68131, Phone 402 498-6561, FAX 402 498-6614, ; Email: richard.tempero@boystown.org

We have no conflicts of interest.

Alitalo, 2010). Mechanisms of angiogenesis are often generalized to lymphangiogenesis, in many cases providing insight and but also potentially jeopardizing the recognition of important distinctions. How proliferating LECs cooperatively assemble to produce a newly synthesized lymphatic vessel *in vivo* remains unclear.

One model of postnatal sprouting angiogenesis requires coordinated and potentially competitive behavior guided by Notch and VEGF gradients to select tip and stalk cells (Blanco and Gerhardt, 2013; Jakobsson et al, 2010; Tammela et al, 2011). In response to VEGF family members, sprouts emerge from preexisting blood endothelial precursors. We use the term precursor generally, to describe a parent ancestor giving rise to progenies or lineages. Precursors proliferate and separate into tip and stalk cells. Proliferating stalk lineages extend the newly synthesized blood vessel and have minimal sprouting because of lateral inhibition by Notch signaling (Lobov et al, 2007). Recent evidence has revealed that VE-cadherin, by mediating tip and stalk cell rearrangement, works to dynamically assemble endothelial cells during angiogenesis (Bentley et al, 2014; Perryn et al, 2008). Far less is known about sprouting lymphangiogenesis. Specifically, do proliferating LEC progenies undergo dynamic rearrangement during lymphangiogenesis and how do proliferating LEC progenies assemble a new lymphatic vessel? To explore these cellular mechanisms, we developed a genetic lineage tracing model to track the fate of lymphatic vessels and small populations of LEC precursors and progeny during experimental manipulation designed to stimulate lymphangiogenesis.

We developed transgenic mice that carried an inducible Cre recombinase-estrogen receptor construct targeted to LECs (Lyve1CreERT2 mice) and crossed these mice to Cg-Gt(ROSA)26Sor $^{tm14(CAG-tdTomato)Hz}$/J) mice carrying a floxed stop tandem dimer tomato (tdT) construct to create Lyve1CreERT2^{tdT} mice. By manipulating the dose and schedule of 4-hydroxytamoxifen (4-OHT) administration in adult Lyve1CreERT2^{tdT} mice, we were able to express tandem dimer tomato (tdT) in entire lymphatic vessels or small populations of LEC precursors, in some cases at a clonal frequency. This strategy allowed us to follow the fate of polyclonal (more than one) or clonal tdT^{+} LEC precursors and progeny during suture induced corneal lymphangiogenesis. In several studies, we used intravital microscopy to directly visualize the tdT^{+} LEC progenies expand in the same mice over the course of 7 days.

The results of the low 4-OHT dose inductive condition were most revealing. tdT^{+} LECs at very low frequency in Lyve1CreERT2^{tdT} mice were stimulated to proliferate using the suture induced model of corneal lymphangiogenesis. Independent of VE-cadherin, we visualized contiguous tdT^{+} LEC progeny assembled to comprise a linear, rather than circumferential, subunit within a newly synthesized tdT^{-} lymphatic vessel. Analysis of this static and dynamic data supports a model of LEC proliferation along the long axis of the vessel and lineage assemblage during lymphangiogenesis.

Results

Inductive genetic strategy for LEC lineage tracing

To investigate the cellular assembly of LECs *in vivo*, we developed a novel inductive genetic strategy to express the fluorescent reporter tandem dimer tomato (tdT) in LECs in adult mice. To target LECs, we generated Lyve1CreERT2 transgenic mice carrying a Cre recombinase-estrogen receptor element driven by a BAC construct containing the LYVE-1 promoter (Figure 1A). Three Lyve1CreERT2 founder strains were crossed with the floxed stop tdT fluorescence reporter strain, B6.Cg-Gt(ROSA)26Sor $^{tm14(CAG-tdT)Hz}$ /J. This reporter strain expresses tdT fluorescence in the presence of activated Cre and has been used to characterize several inductive Cre transgenic systems and lineage studies (Madisen et al, 2010). We generated and tested induction efficiency in the three Lyve1CreERT2^{tdT} strains (Figure 1B). tdT fluorescence was not detected in any strain prior to induction with 4-hydroxytamoxifen (4-OHT). Strain Lyve1CreERT2-49^{tdT} (hereafter referred to as Lyve1CreERT2^{tdT}) demonstrated the greatest and most reliable tdT induction efficiency and was used in all studies. High dose 4-OHT was administered to Lyve1CreERT2^{tdT} mice and the mice were rested for 2 weeks and sacrificed. The tissue was stained with antibodies to LYVE-1. Endogenous tdT fluorescence was readily detected in LYVE-1^{+} lymphatic cells in all tissues examined including skin, corneal limbus, trachea, small intestine (Figures 1C-J) and lymph node, spleen, lung (not shown). We identified differential tdT expression in various tissues and LYVE-1^{+} LECs that were tdT^{-} in Lyve1CreERT2^{tdT} mice treated with high dose 4-OHT. We observed tdT^{+} cells that were LYVE-1^{-}. This may be explained by LYVE-1 expression during induction conditions that then was downregulated or leakiness of the LYVE-1 promotor construct and off target expression. These observations were consistent with the concepts of induction efficiency and tissue to tissue induction variability that are common to these systems (Wendling et al, 2009). The cutaneous tdT^{+} lymphatic vessels appeared to have grossly normal function based upon the ability to transport FITC-dextran (Supplement Figure 1).

Live imaging of newly synthesized corneal lymphatic vessels

The inductive features of this model allowed us to express tdT fluorescence in a population of LEC precursors and track progeny fate during experimental conditions designed to drive proliferation. Cell fate tracking makes use of the principle that the precursor or parent cell passes the modified tdT transgene to all progeny or daughter cells. We used live imaging fluorescent microscopy to follow the fate of polyclonal tdT^{+} LECs during corneal lymphangiogenesis. High dose 4-OHT was administered to Lyve1CreERT^{tdT} mice and the mice were rested for 2 weeks. Corneal sutures were placed to induce lymphangiogenesis and groups of sutured Lyve1CreERT^{tdT} mice were treated with Fc control conditions or VEFG-R2 and –R3 decoy receptors to block the VEGF-A and –C signaling. Live imaging was used to visualize the growth of new lymphatic vessels in real time by sedating the same mouse and performing fluorescent microscopy every other day over the course of 1 week.

For orientation the eyelid, the limbal region, and the cornea are labeled in the first image of Figure 2A. The tdT^{+} signal in the eyelid were cutaneous lymphatic vessels. Serial live imaging revealed tdT^{+} LEC sprouting from the limbal lymphatic and extending centrally in

mice treated with Fc control conditions (Figure 2 panel A). VEFG-R2 and –R3 decoy receptors inhibited lymphatic vessel sprouting, stalk elongation, and the overall process of lymphangiogenesis (Figure 2 panel B and C). Maximum intensity projection (MIP) images obtained using confocal microscopy shows two tdT^+ LYVE-1^+ sprouts. One sprout has MHC II^+ cells interfacing or possibly intravasating into the tip (Figure 2 panel D). The high 4-OHT dose inductive protocol coupled together with live imaging data acquired in individual experimental mice over time allowed us to directly visualize polyclonal tdT^+ LEC sprouting and stalk extension during conditions of new lymphatic vessel growth. Direct acquisition of this data strongly supported the concept that new corneal lymphatic vessel growth developed from a pre-existing LEC precursor within the limbal lymphatic vessel.

Recently, non-venous derived LECs have been identified to directly contribute to cardiac and dermal lymphatic vessels suggesting the presence of a non-venous LEC precursor that functions during lymphangiogenesis (Klotz et al, 2015; Martinez-Corral et al, 2015). Others have described the plasticity of the LYVE-1^+ macrophage population and proposed that these cells directly integrate into new lymphatic vessels (Maruyama et al, 2005; Ran and Montgomery, 2012). In the adult state, LYVE-1 is expressed in LECs and a small population of $CD11b^+$ cells of myeloid lineage, also described as LYVE-1^+ macrophages in the literature (Ran and Montgomery, 2012). Given the use of the LYVE-1 promoter, we anticipated tdT fluorescence expression in cells expressing LYVE-1 at the time of induction such as LYVE-1^+ LECs and macrophages. We visualized tdT fluorescence in single LYVE-1^+ $CD11b^+$ cells in the space posterior to the corneal limbus and the skin. tdT^+ or tdT^- LECs within newly synthesized corneal lymphatic vessels were $CD11b^-$ (Supplement Figure 2), a well-accepted marker of macrophage lineage described to be retained following the differentiation towards the LEC phenotype. Many single $CD11b^+$ cells with macrophage morphology were observed in the inflamed corneal environment suggesting that these cells play an important yet indirect role, for example, expressing VEGF family members (Baluk et al, 2005). Collectively, this data supported a model of proliferating LEC progenies from pre-existing precursors within the limbal lymphatic vessel. Although these findings are not entirely novel, they do not support the model of macrophages differentiating into LECs, and importantly establish a foundation for the LEC small population studies described below.

Kinetics of tdT induction

To investigate the process of proliferation and assembly of LEC progeny, we developed a genetic lineage tracing strategy to follow the fate of tdT^+ LEC precursors within the background of a tdT^- lymphatic vessel. Understanding the kinetics of tdT induction was central to the interpretation of fate mapping and genetic lineage tracing (Ritsma et al, 2013). By directly visualizing the tdT fluorescence using live imaging, we were able to study the kinetics of tdT expression in the corneal limbal lymphatic and confirm the completion of this process at single cell resolution. We used high 4-OHT dose conditions and obtained live images of experimental Lyve1CreERT2^{tdT} mice over time. The tdT fluorescence in the corneal limbal lymphatic vessel was stable and similar between weeks two and three post induction (Supplemental Figure 3A-D). The induction kinetics that we observed were consistent with other published works (Wendling et al, 2009). We developed low 4-OHT dose induction conditions with the primary goal of tdT expression in limbal LEC precursors

at a stable yet extremely rare frequency about 0-2 tdT^+ LECs/cornea. In the image shown, which represents about 20 % of the entire limbal region there is 1 tdT^+ limbal LEC detected by live imaging (Supplemental Figure 3E-G). Although we attempted, it was technically difficult to demonstrate and quantify single tdT^+ LEC precursors using live imaging. The extremely low frequency of the tdT^+ LEC precursors suggested that they were single cell clones.

4-OHT dosing and schedule inductive conditions were modulated to successfully induce a spectrum of tdT^+ expression in Lyve1CreERT2^{tdT} mice with suture induced corneal lymphangiogenesis. Lyve1CreERT2^{tdT} mice were treated with high, intermediate, or low 4-OHT dose inductive conditions and rested for 3 weeks to ensure the completion and stability of tdT expression. The mice were sutured to stimulate corneal lymphangiogenesis. High 4-OHT dose conditions induced tdT in nearly all LYVE-1^+ lymphatic vessels. We interpret this finding such that polyclonal tdT^+ LEC limbal precursors proliferated and produced tdT^+ LEC progenies with a minimal contribution from a tdT^- LEC population (Figure 3A-C). The intermediate 4-OHT dose conditions resulted in a mosaic of tdT^+ and tdT^- LYVE-1^+ lymphatic vessels. We interpret this finding to represent polyclonal tdT^+ and tdT^- LEC precursors proliferating simultaneously to produce a mosaic of tdT^+ and tdT^- LEC progenies (Figure 3D-F). The result from the low 4-OHT dose condition was the most interesting finding. In most cases we identified a single or very few tdT^+ LEC progenies, in which the individual LECs remained grouped and linearly arranged comprising a subunit within a tdT^- LYVE-1^+ lymphatic vessel (Figure 3G-J). Some animals in this group had no tdT^+ progenies, these animals were not useful for data analysis but did help establish the lower limits of the inductive conditions.

We performed additional studies with a similar design to investigate whether lymphatic lineage assemblage persisted as the lymphangiogenesis response matured over time. Lyve1CreERT2^{tdT} mice were treated with intermediate 4-OHT dose inductive conditions and rested for 3 weeks. Lymphangiogenesis was stimulated by suture placement for 2 weeks to allow a more developed lymphangiogenesis response. Lymphatic endothelial lineage assemblage was identified in lymphatic vessels stimulated by inflammation for two weeks (Figure 4 A-E). We counted an average of 1.2 single LYVE-1^+ tdT^+ LECs in 7 corneas compared to an average of 4 groups of LYVE-1^+ tdT^+ LEC progenies containing more than 1 cell. This result was statically significant (Figure 4F). The range of LYVE-1^+ tdT^+ LEC progeny size was highly variable. We interpreted these findings such that a single clone or small population of tdT^+ LEC precursors proliferated but the tdT^+ LEC lineage remained closely assembled comprising a subunit of a larger lymphatic vessel. Lineage assemblage was a surprising finding. We thought this was inconsistent with the dynamic endothelial shuffling models which would predict a diffuse rearrangement of tdT^+ LECs throughout the entire newly synthesized lymphatic vessel.

LEC lineage assemblage was independent of VE-cadherin

Endothelial shuffling and rearrangement has been shown to be dependent upon VE-cadherin. We investigated whether VE-cadherin blockade would potentiate or inhibit LEC lineage assemblage. We anticipated a negative result in this study. In preliminary studies we used the

suture induced model of corneal inflammation to stimulate new lymphatic vessel growth in 129/SV mice and treated groups of mice with neutralizing antibodies to VE-cadherin or isotype control antibodies administered subconjunctively. This route, rather than systemic injection, was selected based on the published toxicity following systemic administration of VE-cadherin neutralizing antibodies, in particular clone BV13 (Corada et al, 1999). C57/BL6 and 129/SV mice treated with VE-cadherin blocking antibodies survived and did not develop signs of distress (**data not shown**). These mice developed significantly more lymphatic vessel loops compared to isotype control treated mice (Figure 5A-C), although the overall lymphatic vessel density and number of sprouts did not change (Figure 5D and E). Suture placement and control antibody injection conditions increased mRNA levels of MMP-10, IL-1a, IL-6, NGF, VEGF-A and VEGF-C, although the increases in IL-6, VEGF-A, and VEGF-C were not statistically significant in both C57/BL6 and 129/SV strains. Both C57/BL6 and 129/SV backgrounds were studied as both strains were used in this manuscript. In general, we quantified higher mRNA levels in the 129/SV mice compared to the C57/BL6 mice. Of these molecules, VE-cadherin blockade inhibited only MMP-10 significantly (Supplement Figure 4). The results suggested that VE-cadherin neutralizing antibodies were not regulating the VEGF family members nor stimulating a more robust inflammatory response as levels of IL-1a and IL-6 remained stable. Unlike corneal burn or transplantation models (Hajrasouliha et al, 2012), VEGF-C mRNA levels do not increase during suture induced inflammatory lymphangiogenesis (Fink et al, 2014;Kelley et al, 2011;Kelley et al, 2013). MMP-10 expression mediated by β1 integrins has been identified by our laboratory to be pro-lymphangiogenic (Steele et al, 2011); however, at this time the exact relationship between VE-cadherin and MMP-10 is unclear.

Next, we designed genetic lineage tracing studies to investigate the role of VE-cadherin in LEC lineage assemblage. Low 4-OHT dose conditions were administered to Lyve1CreERT2^{tdT} mice to induce tdT fluorescence expression in a low frequency of LEC precursors and these mice were rested for 3 weeks. Lymphangiogenesis was stimulated by corneal suture placement and groups of mice were treated with either VE-cadherin blocking antibodies or isotype control antibodies. After 1 week the mice were scarified and the tissue processed. Low power epifluorescent microscopy showed none, one, or two groups of LYVE-1$^+$ tdT$^+$ LEC progeny per corneal hemisection. MIP images obtained using confocal microscopy showed tdT$^+$ LEC progeny contiguously and linearly within a LVYE-1$^+$ lymphatic vessel in the isotype control conditions (Figure 6A-C). Similar analysis showed contiguous tdT$^+$ LEC progeny arranged in a LYVE-1$^+$ lymphatic vessel in mice treated with VE-cadherin blocking antibodies (Figure 6D-F). LEC progeny size was similar suggesting that the VE-cadherin blockade did not affect the proliferative capacity of these cells (Figure 6G) and the individual size of the tdT$^+$ LECs in both groups was similar (Figure 6H). These findings provide additional support for LEC lineage assemblage model.

LEC proliferative characteristics in vivo

Initially, we showed that phospho histone H3 staining was localized to the stalk rather than the tip or limbal structures in newly synthesized lymphatic vessels (Figure 7A and B). This provided additional support for lymphatic vessel stalk proliferation. Next, we investigated the angle of the LEC mitotic cleavage plane relative to the long axis of the lymphatic vessel.

Using a blood endothelia model, the mitotic cleavage plane orthogonally oriented to the long axis of the vessel has been correlated with the direction of vessel growth (Zeng et al, 2007). We measured the mitotic plane of proliferating LYVE-1$^+$, tdT$^+$, and DAPI$^+$ LECs cells relative to the long axis of newly synthesized lymphatic vessels in corneal tissue from Lyve1CreERT2^{tdT} mice treated with high 4-OTH inductive conditions. The results showed that more than 70% of the proliferating LECs had a mitotic cleavage plane 70-90 degrees relative to the long axis of the lymphatic vessel (Figure 8A-C).

Discussion

We have shown that LEC progeny maintain a contiguous relationship during lymphangiogenesis by following the fates of genetically labeled LEC precursors *in vivo*. We developed an inductive Cre-lox system to drive expression of a tdT fluorescent reporter in LECs. By modulating the 4-OHT schedule and dose conditions, we were able to temporally and quantitatively control the tdT fluorescence expression in LEC precursors in adult mice. We coupled this system to a corneal model of inflammatory lymphangiogenesis and tracked the fate of proliferating polyclonal or small populations of tdT$^+$ LEC precursors, in some cases directly visualizing these events using live imaging techniques. Interpretation of this dynamic and static data supports a model of lymphatic endothelial lineage assemblage. Based upon these direct *in vivo* observations, lymphatic endothelial lineage assemblage is a conceptually novel finding that appears to be in diametric contrast to the proposed endothelial shuffling and rearrangement model.

Recently, genetic lineage tracing strategies using combinations of inducible recombinase systems and fluorescent reporter constructs has provided valuable insight towards the basic questions of epithelial (Doupe et al, 2012;Mascre et al, 2012;Schepers et al, 2012;Snippert et al, 2010;Zeng et al, 2007;Clayton et al, 2007), mesenchymal (Rinkevich et al, 2011;Rinkevich et al, 2012), and hematopoietic (Schraml et al, 2013) biology, homeostasis, and stemness properties. Within the field of lymphatic vessel biology, lineage tracing established the venous origin of the lymphatic vasculature (Srinivasan et al, 2007). More recently, studies featuring an inductive Prox1-Cre-ERT2 system have shown how LECs migrate during embryogenesis to form valve structures within lymphatic vessels (Bazigou et al, 2011;Tatin et al, 2013) and the potential applications of inductive genetic reporter systems in the lymphatic vasculature (Bianchi et al, 2015). The Lyve1CreERT2 strain described here may be a valuable resource to investigators interested in regulating gene expression in lymphatic vessels.

The studies presented in this manuscript use the Lyve1CreERT2 strain and genetic lineage tracing techniques to explore for the first time the fate of newly synthesized LECs during disease induced lymphangiogenesis. Successful interpretation of all genetic lineage tracing studies is based on the principle that the modified transgene is passed to all progeny during cell proliferation (Kretzschmar and Watt, 2012). We developed live imaging techniques and directly visualized that tdT expression was complete and stable 2 weeks after 4-OHT administration in adult Lyve1CreERT2^{tdT} mice. These *in vivo* observations enabled us to directly visualize, rather than infer, that accumulation of tdT$^+$ LECs were a result of proliferation and passage of modified tdT transgene rather than lingering inductive

conditions. These direct observations guided the timing of lineage tracing experiments. We chose to develop the lymphatic lineage tracing strategies because many other techniques, such as tritiated thymidine uptake *in vivo* and pHH3 staining label proliferating cells in a non-specific manner (shown in Figure 7). This can make it difficult to discern the cell population of interest from other proliferating populations, such as blood endothelia and leukocytes, both of which are well known proliferating constituents of an inflammatory disease model.

Phototoxicity is an emerging concern in fluorescent microscopy experiments (Carlton et al, 2010). We recognized phototoxic conditions in preliminary studies using magnification greater than 200×. The associated dose of irradiation bleached the tdT fluorescence and seemed to cause permanent changes to cell surface molecules. We acquired data well below the phototoxic threshold. Using the described live imaging conditions, we did not detect recognizable changes in tdT fluorescence, cell surface antigen expression, or tissue changes.

Recently, cardiac and dermal lymphatic vessels have been identified using lineage tracing techniques to harbor venous and non-venous derived LECs (Klotz et al, 2015; Martinez-Corral et al, 2015). The implication of this finding is the presence of a non-venous LEC precursor that functions during developmental and pathological lymphangiogenesis. We considered these recent reports and other reports that described the plasticity of the LYVE-1$^+$ macrophage population and the hypothesis that these cells directly integrate into new lymphatic vessels (Maruyama et al, 2005; Ran and Montgomery, 2012). We did see very few, less than 1%, tdT$^+$ LYVE-1$^+$, CD11b$^+$ cells in the lymphatic vessels. Given the low frequency of these cells and the inability to distinguish whether these cells were integrated into vessel wall, within the lymphatic vessel lumen, or in the corneal microenvironment, we were unable to generate convincing data to support that a non-venous derived cell, such as a macrophage, integrated directly into newly synthesized corneal lymphatic vessels. We remain open to this possibly, particularly as loss of cell surface markers or transdifferentiation can make the identification of such cells challenging. The system used in these studies is not an ideal model to lineage trace LYVE-1$^+$ macrophages in that a LYVE-1$^+$ macrophages may express tdT following 4-OHT treatment. This makes it potentially difficult to discriminate between tdT$^+$ LECs and tdT$^+$ macrophages. We concluded that the primary mechanism of suture induced corneal lymphangiogenesis was proliferation of preexisting LEC precursors from the limbus.

We developed low 4-OHT dose inductive conditions such that we could induce tdT expression in a very low frequency of tdT$^+$ LEC precursors and follow the lineage or progeny expand within a newly synthesized tdT$^-$ lymphatic vessel. This feature is unique and separates this inductive model from constitutive reporter systems. We were able to develop inductive conditions such that only one or two tdT$^+$ LEC precursors and resultant progenies were detected per corneal hemi section. This low progeny frequency suggested an origin from clonal tdT$^+$ LEC precursor, although this was difficult to establish conclusively. Although we attempted, it was impractical and technically difficult to use serial live imaging techniques to visualize single tdT$^+$ LEC progenies. In these studies, we visualized infrequent tdT$^+$ tip cells, too few to quantify. Whether this observation represents biologic event or is a consequence of intended low frequency tdT expression is unclear.

VE-Cadherin mediated dynamic endothelial cell shuffling and rearrangement during angiogenesis has been shown (Bentley et al, 2014;Jakobsson et al, 2010;Arima et al, 2011). This well developed angiogenesis model is based largely upon *in vitro* studies using embryoid bodies, zebrafish organogenesis models, and mouse retinal studies using 'snap shot' histologic or indirect measurements. The endothelial cell shuffling model would predict lineage dissociation resulting in a random rearrangement of individual LECs throughout the newly synthesized lymphatic vessels. We did not observe such findings. We observed that independent of VE Cadherin blockade, small populations of tdT^+ precursors stimulated to proliferate resulted in tdT^+ lymphatic endothelial lineages that were assembled contiguously with apparent cell to cell contact. The junctional properties of lymphatic vessels have been studied. Newly synthesized lymphatic capillaries express VE-cadherin, a major component of the adherens junction, diffusely. Later in time, VE-cadherin becomes clustered to generate a 'button' phenotype (Yao et al, 2012). In reconciling these observations with the data presented here, it is interesting to consider that LEC progeny may change the spatial expression of VE-cadherin as part of a vessel maturation process. Although we did not determine whether the LECs within an assemblage were adherent, the results suggest that the lineage assemblage process was unrelated to VE-cadherin. A technical limitation of the VE-Cadherin neutralizing antibodies used in this approach is also a possible explanation for these results. Whether lineage assemblage is unique to the lymphatic vasculature or a product of the direct *in vivo* experimental strategies used in this manuscript is unclear at this time.

In many cases, tdT^+ LEC progeny did not extend the entire length of the newly synthesized lymphatic vessel. In groups of mice treated with the VE-cadherin neutralizing or control antibodies, the average tdT^+ LEC progeny size was 10 cells. This is potentially similar to the work of others that showed VE-cadherin stabilized new blood vessels but does not regulate their proliferation (Crosby et al, 2005). In the studies in which we allowed the lymphangiogenesis to develop over two weeks, the progenies had a wide range of tdT^+ LECs from 2 to over 100. Aside from the major finding of lymphatic endothelial lineage assemblage, the size of the LEC lineage is intriguing. One interpretation of this data is that all LECs (precursors) have a capacity to proliferate; however, the proliferative capacity is highly variable. These observation raise intriguing questions for future study: i) do all LECs have the same proliferative capacity? ii) if not, what is the mechanism underlying this cell fate/lineage decision process? and iii) is the LEC proliferative capacity exhaustive, and iv) are the LEC assemblages related to LEC specialization such as branching, anastamosis, or function?

Based on these dynamic and static observations, we propose a lymphatic endothelial lineage assemblage model in which LEC precursors proliferate and their progeny maintain an assemblage arranged within a new lymphatic vessel (Figure 9). These findings raise new and fundamental questions regarding LEC precursor and progeny cell fate decisions and endothelial population dynamics during lymphangiogenesis.

Materials and methods

All animal protocols were approved by Boys Town National Research Hospital Institutional Animal Care and Use Committee institutional review board in accordance with NIH guidelines.

Mouse strains

To create the Lyve1CreERT2^{tdT} mice, the CreERT2 construct, a hybrid molecule containing a CRE domain fused to the estrogen ligand binding domain, was inserted into a bacterial artificial chromosome (BAC) containing the LYVE-1 promoter and gene. The mouse BAC RP23 332E15 which contains the LYVE-1 gene flanked by approximately 100 kb on both sides was obtained from a collection maintained by the Children's Hospital Oakland Research Institute. The plasmid pCreERT2K12Kan was a generous gift from Professor P. Chambon (IGBMC, Illkirch, France). Left (LHA) and right (RHA) homology arms were synthesized using LYVE-1 derived adapter primers which allowed directed cloning into the pCreERT2K12Kan vector. The BAC RP23 332E115 was recombined with the pCreERT2K12Kan containing the LYVE-1 homology arms in the recombineering strain SW102 (NCI). The PKGNeo cassette flanked by FRT sites was removed using the recombineering strain SW105 (NCI). The BAC 332E15-LYVE-1-pCreERT2 was characterized by direct sequencing and by PCR amplification with primers that span the 5' and 3' junctions of the LYVE-1 gene and the transgene (pCreERT2). Five strains of mice transgenic for Lyve1CreERT2 were generated at the University of Michigan Gene Targeting Facility. Three strains transmitted the transgene in the germline after crossing with C57BL/6 (Charles River). The transgenic strains are maintained in the hemizygous state by crossing to C57BL/6. After 12 generations of such crosses, the three strains were crossed to Cg-Gt(ROSA)26Sor $^{tm14(CAG-tdTomato)Hz}$/J) F1 mice (Jackson Laboratories, Bar Harbor, Maine) to create Lyve1CreERT2-49^{tdT}, Lyve1CreERT2-54^{tdT}, and Lyve1CreERT2-60^{tdT} strains. 129/SV mice were purchased from Charles River (Wilmington, MA).

Corneal mouse model of suture induce inflammation

The corneal model of suture induced inflammation was described previously (Kelley et al, 2011). These techniques were used to induce corneal inflammation and stimulate new lymphatic vessel growth in age matched Lyve1CreERT2^{tdT} and 129/SV mice.

4-OHT induction protocols

For high dose induction, 1 mg 4-OHT suspended in sunflower oil was administered intraperitoneally on three consecutive days. For intermediate dose induction, 1 mg 4-OHT suspended in sunflower oil was administered intraperitoneally. For low dose induction, 0.25 or 0.5 mg 4-OHT suspended in sunflower oil was administered intraperitoneally.

Injection of decoy receptors or blocking antibodies

Lyve1CreERT2^{tdT} or 129SV mice were injected with 20 μl (1mg/ml) rat anti-VE-cadherin antibody (16-144-85 eBioscience, San Diego, CA) or a Rat IgG1 isotype control (16-4301-85 eBioscience) into the subconjunctival space of the eye at the day suturing (day = 0) and at day 3 and day 5. At day 7 cornea were isolated, fixed and prepared for

immunofluorescent microscopy as previously described (Kelley et al, 2013). A similar protocol was used with either a cocktail of VEGF-R2-Fc and -R3-Fc decoy receptors or their respective control Fc as previously described (Kelley et al, 2013).

Real time analysis of corneal mRNA

mRNA for specific transcripts were quantified by TaqMan-based real-time PCR as previously described (Steele et al, 2011). The following mouse TaqMan primer sets were used: MMP-10 (Mm00444630_m1), IL-1a (Mm00439620_m1), NGF (Mm00443039_m1), VEGF-A (Mm01281449_m1), IL-6 (Mm00446190_m1), and VEGF-C (Mm00437310_m1) (ThermoFisher Scientific, Waltham, MA).

Microscope image acquisition

All images were acquired at ambient temperature: approximately 23°C.

Live imaging

Live imaging was performed on sedated Lyve1CreERT^{tdT} mice. The mouse was positioned laterally and the globe exposed by retracting the eyelids to expose the limbus near the lateral canthus. Images were obtained using a Leica MZ10F Fluo III microscope using a Leica Planap 1.0× objective and a Leica DFC310FX camera (acquisition software: LAS version 4.0.0.8777) or a Ziess Axio Zoom.V16 and a Zeiss Plan-NeofluarZ 1.0 0.25 na objective and a Zeiss AxioCam MRm camera (acquisition software: Zeiss Zen 2012, blue edition, version 1.1.1.0).

Epifluorescence microscopy

Epifluorescent images were acquired using a Zeiss Axio-Imager.A1 and an EC Plan-Neofluar 10× 0.3 na objective and a Diagnostic Instruments SpotFlex model 15.2 64 Mp Shifting Pixel camera (acquisition software: SPOT windows version 4.6 or 5.1).

Confocal Microscopy

Confocal images were acquired on either a Leica TCS SP8 MP (Creighton University Integrated Biomedical Imaging Facility) using either a HC PL Apochromat 20× 0.75 na objective or a HC PL Apochromat 40× 1.3 na oil objective (acquisition software: Leica LAS AF version 3.2.1.9702, 12 bit) or a Zeiss AxioObserver LSM 710 (University of Nebraska Medical Center Confocal Laser Scanning Microscope Core Facility) using either a Plan-Apochromat 20× 0.8 na objective or an EC Plan-Neofluar 40× 1.30 na oil objective (acquisition software: Zeiss Zen 2011).

Processing software

Cropping, channel separation, orthogonal and maximum intensity projections were done in the FIGI version of ImageJ (1.47v) or in the respective confocal acquisition software. Stitching of confocal images was done using the Stitching Plug-In in Image J (Preibisch et al, 2009), or in the respective confocal acquisition software. Figures were prepared from original images in Adobe Photoshop.

Tissue staining and antibodies

To visualize lymphatic vessels within their microenvironment and study specific features that were identified during live imaging, cornea tissues were fixed in 1% paraformaldehyde in PBS pH 7.4 and labeled as previously described using whole mount techniques (Kelley et al, 2013). Whole mount mouse cornea, pinna, small intestine, trachea was stained with antibodies to LYVE-1 (11-034, AngioBio, Del Mar, CA), CD31 (MAB1398Z, EMD Millipore, Billerica, MA), pHH3 (H9908, Sigma-Alrich, St. Louis, MO), CD11b (13-0112-81, eBioscience), MHCII (13-5321-81, eBioscience), DAPI (Sigma-Aldrich) and the appropriate secondary antibody: using the fluorochromes Alexa488, Alexa555, Alexa633 (ThermoFisher Scientific) and DyLight488 (Jackson ImmunoResearch Laboratories, West Grove, PA). Fixed and labeled whole mounts were mounted in Vectashield H-1000 (Vector Laboratories, Burlingame, CA).

Uptake of dextran fluorescein

Lyve1CreERT^{tdT} mice were induced with the high 4-OHT protocol and rested for 2 weeks. 2 μl of lysine fixable dextran fluorescein 2,000,000 MW anionic (D-7137, ThermoFisher Scientific) was microinjected into the margin of the pinna of sedated Lyve1CreERT^{tdT} mice. After 20 minutes the tissue was collected and fixed with 1% PFA and analyzed.

Morphologic measurements of lymphatic vessels and cells

These techniques were described previously (Steele et al, 2011). Briefly, we recorded immunofluorescence (IF) images from corneas using a Zeiss Axio Imager A.1 microscope (for epifluoresence) or a Zeiss LSM510 META confocal microscope. For each corneal epifluorescence image, we overlaid a customized rectangular grid adjacent to the constitutive limbal lymphatic vessels. The grid consisted of 250 square boxes. Each box measured 115 μm^2. For lymphatic density measurements, we counted the number of grid squares occupied by a lymphatic vessel wall, lumen, or sprout. We expressed this data as number of occupied grid squares (relative area) ±SD. We quantified the number of lymphatic vessel sprouts or loops within the grid. We defined a vessel sprout as a terminal conical projection with a length of at least 10 microns and a loop as a circular vessel structure. For progeny size measurements we simply counted the number of individual tdT$^+$ LECs within a given lineage. To quantify individual tdT$^+$ LEC size, the cell size visualized high resolution MIP was measured in two dimensions using standard tools in Image J. The product was expressed in μm^2.

pHH3 and LYVE-1 localization studies

Lymphangiogenesis was stimulated in SV/129 mice using the suture induced model of corneal inflammation. Corneas were labeled with antibodies to LYVE-1 and pHH3. Single z plane images were obtained using confocal microscopy from 14 individual mice. Random fields containing LYVE-1$^+$ lymphatic vessels were identified and the localization of the pHH3 staining (limbus, branch, tip) was quantified.

Statistical Analysis

Whisker plots show standard deviation. The unpaired student T test was used to evaluate statistical significance in studies with two groups. P value less than 0.05 was considered significant. The presence of a bracket between groups indicates statistical significance.

Supplementary Material

Refer to Web version on PubMed Central for supplementary material.

ACKNOWLEDGEMENTS

This work was funded by grants from NIH: National Eye Institute RO1-EY021571 and National Institute of General Medical Sciences, 5 P20 RR018788-08. Part of this research was conducted at the Integrative Biological Imaging Facility at Creighton University, Omaha, NE (Leica TCS SP8 MP). This facility, supported by the Creighton University School of Medicine was constructed with support from grants from the National Center for Research Resources (5P20RR016469) and the National Institute for General Medical Science (NIGMS) (8P20GM103427), a component of the National Institutes of Health (NIH). Microscope Core Facility at the University of Nebraska Medical Center for providing assistance with confocal microscopy and the Nebraska Research Initiative and the Eppley Cancer Center for their support of the Core Facility (Zeiss LSM 710). This investigation is solely the responsibility of the authors and does not necessarily represent the official views of NIGMS or NIH. We acknowledge Maggie Van Keuren for preparation of transgenic mice and the Transgenic Animal Model Core of the University of Michigan's Biomedical Research Core Facilities.

Abbreviation List

LECs	lymphatic endothelial cells
tdT	tandem dimer tomato
na	numeric aperture
MIP	maximum intensity projection

Reference List

Alitalo K. The lymphatic vasculature in disease. Nat Med. 2011; 17:1371–1380. [PubMed: 22064427]

Arima S, Nishiyama K, Ko T, Arima Y, Hakozaki Y, Sugihara K, Koseki H, Uchijima Y, Kurihara Y, Kurihara H. Angiogenic morphogenesis driven by dynamic and heterogeneous collective endothelial cell movement. Development. 2011; 138:4763–4776. [PubMed: 21965612]

Baluk P, Tammela T, Ator E, Lyubynska N, Achen MG, Hicklin DJ, Jeltsch M, Petrova TV, Pytowski B, Stacker SA, Yla-Herttuala S, Jackson DG, Alitalo K, McDonald DM. Pathogenesis of persistent lymphatic vessel hyperplasia in chronic airway inflammation. J Clin Invest. 2005; 115:247–257. [PubMed: 15668734]

Bazigou E, Lyons OT, Smith A, Venn GE, Cope C, Brown NA, Makinen T. Genes regulating lymphangiogenesis control venous valve formation and maintenance in mice. J Clin Invest. 2011; 121:2984–2992. [PubMed: 21765212]

Bentley K, Franco CA, Philippides A, Blanco R, Dierkes M, Gebala V, Stanchi F, Jones M, Aspalter IM, Cagna G, Westrom S, Claesson-Welsh L, Vestweber D, Gerhardt H. The role of differential VE-cadherin dynamics in cell rearrangement during angiogenesis. Nat Cell Biol. 2014; 16:309–321. [PubMed: 24658686]

Bianchi R, Teijeira A, Proulx ST, Christiansen AJ, Seidel CD, Rulicke T, Makinen T, Hagerling R, Halin C, Detmar M. A Transgenic Prox1-Cre-tdTomato Reporter Mouse for Lymphatic Vessel Research. PLoS One. 2015; 10:e0122976. [PubMed: 25849579]

Blanco R, Gerhardt H. VEGF and Notch in tip and stalk cell selection. Cold Spring Harb Perspect Med. 2013; 3:a006569. [PubMed: 23085847]

Carlton PM, Boulanger J, Kervrann C, Sibarita JB, Salamero J, Gordon-Messer S, Bressan D, Haber JE, Haase S, Shao L, Winoto L, Matsuda A, Kner P, Uzawa S, Gustafsson M, Kam Z, Agard DA, Sedat JW. Fast live simultaneous multiwavelength four-dimensional optical microscopy. Proc Natl Acad Sci U S A. 2010; 107:16016–16022. [PubMed: 20705899]

Clayton E, Doupe DP, Klein AM, Winton DJ, Simons BD, Jones PH. A single type of progenitor cell maintains normal epidermis. Nature. 2007; 446:185–189. [PubMed: 17330052]

Corada M, Mariotti M, Thurston G, Smith K, Kunkel R, Brockhaus M, Lampugnani MG, Martin-Padura I, Stoppacciaro A, Ruco L, McDonald DM, Ward PA, Dejana E. Vascular endothelial-cadherin is an important determinant of microvascular integrity in vivo. Proc Natl Acad Sci U S A. 1999; 96:9815–9820. [PubMed: 10449777]

Crosby CV, Fleming PA, Argraves WS, Corada M, Zanetta L, Dejana E, Drake CJ. VE-cadherin is not required for the formation of nascent blood vessels but acts to prevent their disassembly. Blood. 2005; 105:2771–2776. [PubMed: 15604224]

Doupe DP, Alcolea MP, Roshan A, Zhang G, Klein AM, Simons BD, Jones PH. A single progenitor population switches behavior to maintain and repair esophageal epithelium. Science. 2012; 337:1091–1093. [PubMed: 22821983]

Fink DM, Connor AL, Kelley PM, Steele MM, Hollingsworth MA, Tempero RM. Nerve growth factor regulates neurolymphatic remodeling during corneal inflammation and resolution. PLoS One. 2014; 9:e112737. [PubMed: 25383879]

Hajrasouliha AR, Funaki T, Sadrai Z, Hattori T, Chauhan SK, Dana R. Vascular endothelial growth factor-C promotes alloimmunity by amplifying antigen-presenting cell maturation and lymphangiogenesis. Invest Ophthalmol Vis Sci. 2012; 53:1244–1250. [PubMed: 22281820]

Jakobsson L, Franco CA, Bentley K, Collins RT, Ponsioen B, Aspalter IM, Rosewell I, Busse M, Thurston G, Medvinsky A, Schulte-Merker S, Gerhardt H. Endothelial cells dynamically compete for the tip cell position during angiogenic sprouting. Nat Cell Biol. 2010; 12:943–953. [PubMed: 20871601]

Karpanen T, Alitalo K. Molecular biology and pathology of lymphangiogenesis 11. Annu Rev Pathol. 2008; 3:367–397. [PubMed: 18039141]

Kelley PM, Connor AL, Tempero RM. Lymphatic vessel memory stimulated by recurrent inflammation. Am J Pathol. 2013; 182:2418–2428. [PubMed: 23578386]

Kelley PM, Steele MM, Tempero RM. Regressed lymphatic vessels develop during corneal repair. Lab Invest. 2011; 91:1643–1651. [PubMed: 21863060]

Klotz L, Norman S, Vieira JM, Masters M, Rohling M, Dube KN, Bollini S, Matsuzaki F, Carr CA, Riley PR. Cardiac lymphatics are heterogeneous in origin and respond to injury. Nature. 2015; 522:62–67. [PubMed: 25992544]

Kretzschmar K, Watt FM. Lineage tracing. Cell. 2012; 148:33–45. [PubMed: 22265400]

Lobov IB, Renard RA, Papadopoulos N, Gale NW, Thurston G, Yancopoulos GD, Wiegand SJ. Delta-like ligand 4 (Dll4) is induced by VEGF as a negative regulator of angiogenic sprouting. Proc Natl Acad Sci U S A. 2007; 104:3219–3224. [PubMed: 17296940]

Madisen L, Zwingman TA, Sunkin SM, Oh SW, Zariwala HA, Gu H, Ng LL, Palmiter RD, Hawrylycz MJ, Jones AR, Lein ES, Zeng H. A robust and high-throughput Cre reporting and characterization system for the whole mouse brain. Nat Neurosci. 2010; 13:133–140. [PubMed: 20023653]

Martinez-Corral I, Ulvmar MH, Stanczuk L, Tatin F, Kizhatil K, John SW, Alitalo K, Ortega S, Makinen T. Nonvenous origin of dermal lymphatic vasculature. Circ Res. 2015; 116:1649–1654. [PubMed: 25737499]

Maruyama K, Ii M, Cursiefen C, Jackson DG, Keino H, Tomita M, van RN, Takenaka H, D'Amore PA, Stein-Streilein J, Losordo DW, Streilein JW. Inflammation-induced lymphangiogenesis in the cornea arises from CD11b-positive macrophages. J Clin Invest. 2005; 115:2363–2372. [PubMed: 16138190]

Mascre G, Dekoninck S, Drogat B, Youssef KK, Brohee S, Sotiropoulou PA, Simons BD, Blanpain C. Distinct contribution of stem and progenitor cells to epidermal maintenance. Nature. 2012; 489:257–262. [PubMed: 22940863]

Perryn ED, Czirok A, Little CD. Vascular sprout formation entails tissue deformations and VE-cadherin-dependent cell-autonomous motility. Dev Biol. 2008; 313:545–555. [PubMed: 18062955]

Preibisch S, Saalfeld S, Tomancak P. Globally optimal stitching of tiled 3D microscopic image acquisitions. Bioinformatics. 2009; 25:1463–1465. [PubMed: 19346324]

Ran S, Montgomery KE. Macrophage-mediated lymphangiogenesis: the emerging role of macrophages as lymphatic endothelial progenitors. Cancers (Basel). 2012; 4:618–657. [PubMed: 22946011]

Rinkevich Y, Lindau P, Ueno H, Longaker MT, Weissman IL. Germ-layer and lineage-restricted stem/progenitors regenerate the mouse digit tip. Nature. 2011; 476:409–413. [PubMed: 21866153]

Rinkevich Y, Mori T, Sahoo D, Xu PX, Bermingham JR Jr. Weissman IL. Identification and prospective isolation of a mesothelial precursor lineage giving rise to smooth muscle cells and fibroblasts for mammalian internal organs, and their vasculature. Nat Cell Biol. 2012; 14:1251–1260. [PubMed: 23143399]

Ritsma L, Steller EJ, Ellenbroek SI, Kranenburg O, Borel Rinkes IH, van RJ. Surgical implantation of an abdominal imaging window for intravital microscopy. Nat Protoc. 2013; 8:583–594. [PubMed: 23429719]

Schepers AG, Snippert HJ, Stange DE, van den Born M, Van Es JH, van de Wetering M, Clevers H. Lineage tracing reveals Lgr5+ stem cell activity in mouse intestinal adenomas. Science. 2012; 337:730–735. [PubMed: 22855427]

Schraml BU, van BJ, Zelenay S, Whitney PG, Filby A, Acton SE, Rogers NC, Moncaut N, Carvajal JJ, Reis e Sousa. Genetic tracing via DNGR-1 expression history defines dendritic cells as a hematopoietic lineage. Cell. 2013; 154:843–858. [PubMed: 23953115]

Snippert HJ, van der Flier LG, Sato T, Van Es JH, van den Born M, Kroon-Veenboer C, Barker N, Klein AM, van RJ, Simons BD, Clevers H. Intestinal crypt homeostasis results from neutral competition between symmetrically dividing Lgr5 stem cells. Cell. 2010; 143:134–144. [PubMed: 20887898]

Srinivasan RS, Dillard ME, Lagutin OV, Lin FJ, Tsai S, Tsai MJ, Samokhvalov IM, Oliver G. Lineage tracing demonstrates the venous origin of the mammalian lymphatic vasculature. Genes Dev. 2007; 21:2422–2432. [PubMed: 17908929]

Steele MM, Schieler AM, Kelley PM, Tempero RM. beta1 integrin regulates MMP-10 dependant tubulogenesis in human lymphatic endothelial cells. Matrix Biol. 2011; 30:218–224. [PubMed: 21406228]

Tammela T, Alitalo K. Lymphangiogenesis: Molecular mechanisms and future promise. Cell. 2010; 140:460–476. [PubMed: 20178740]

Tammela T, Zarkada G, Nurmi H, Jakobsson L, Heinolainen K, Tvorogov D, Zheng W, Franco CA, Murtomaki A, Aranda E, Miura N, Yla-Herttuala S, Fruttiger M, Makinen T, Eichmann A, Pollard JW, Gerhardt H, Alitalo K. VEGFR-3 controls tip to stalk conversion at vessel fusion sites by reinforcing Notch signalling. Nat Cell Biol. 2011; 13:1202–1213. [PubMed: 21909098]

Tatin F, Taddei A, Weston A, Fuchs E, Devenport D, Tissir F, Makinen T. Planar cell polarity protein Celsr1 regulates endothelial adherens junctions and directed cell rearrangements during valve morphogenesis. Dev Cell. 2013; 26:31–44. [PubMed: 23792146]

Wendling O, Bornert JM, Chambon P, Metzger D. Efficient temporally-controlled targeted mutagenesis in smooth muscle cells of the adult mouse. Genesis. 2009; 47:14–18. [PubMed: 18942088]

Wuest TR, Carr DJ. VEGF-A expression by HSV-1-infected cells drives corneal lymphangiogenesis 1. J Exp Med. 2010; 207:101–115. [PubMed: 20026662]

Yao LC, Baluk P, Feng J, McDonald DM. Steroid-Resistant Lymphatic Remodeling in Chronically Inflamed Mouse Airways. Am J Pathol. 2010

Yao LC, Baluk P, Srinivasan RS, Oliver G, McDonald DM. Plasticity of button-like junctions in the endothelium of airway lymphatics in development and inflammation. Am J Pathol. 2012; 180:2561–2575. [PubMed: 22538088]

Zeng G, Taylor SM, McColm JR, Kappas NC, Kearney JB, Williams LH, Hartnett ME, Bautch VL. Orientation of endothelial cell division is regulated by VEGF signaling during blood vessel formation. Blood. 2007; 109:1345–1352. [PubMed: 17068148]

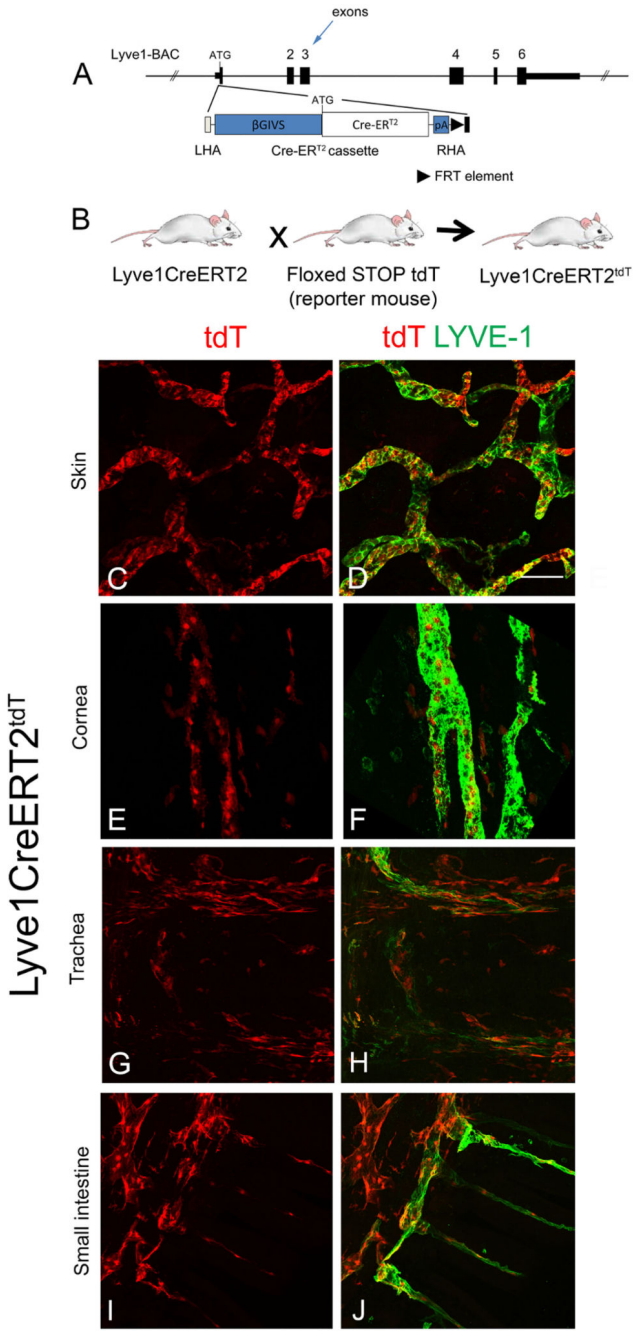

Figure 1.

Inducible tdT fluorescence in Lyve1CreERT2^{tdT} tissue. A schematic is shown representing the Cre recombinase-estrogen receptor construct used to generate the Lyve1CreERT2 mice (A). Mice transgenic for the Lyve1CreERT2 construct were crossed with a Cre reporter strain, Cg-Gt(ROSA)26Sor tm14(CAG-tdTomato)Hz/J), to generate Lyve1CreERT2^{tdT} mice (B). In the absence of 4-OHT, tdT fluorescence expression was not detected in Lyve1CreERT2^{tdT} strains. Lyve1CreERT2^{tdT} mice were induced with high dose 4-OHT, rested for two weeks, and the tissues were harvested. Maximum intensity projection images

obtained using confocal microscopy of skin (C and D), corneal limbus (E and F), trachea (G and H), and small intestine (I and J) showed endogenous tdT expression in LYVE-1^+ lymphatic vessels. The data shown are representative of 4 independent studies, with 3-4 mice per study. All images are 200× and the size standard in D is 200 μm.

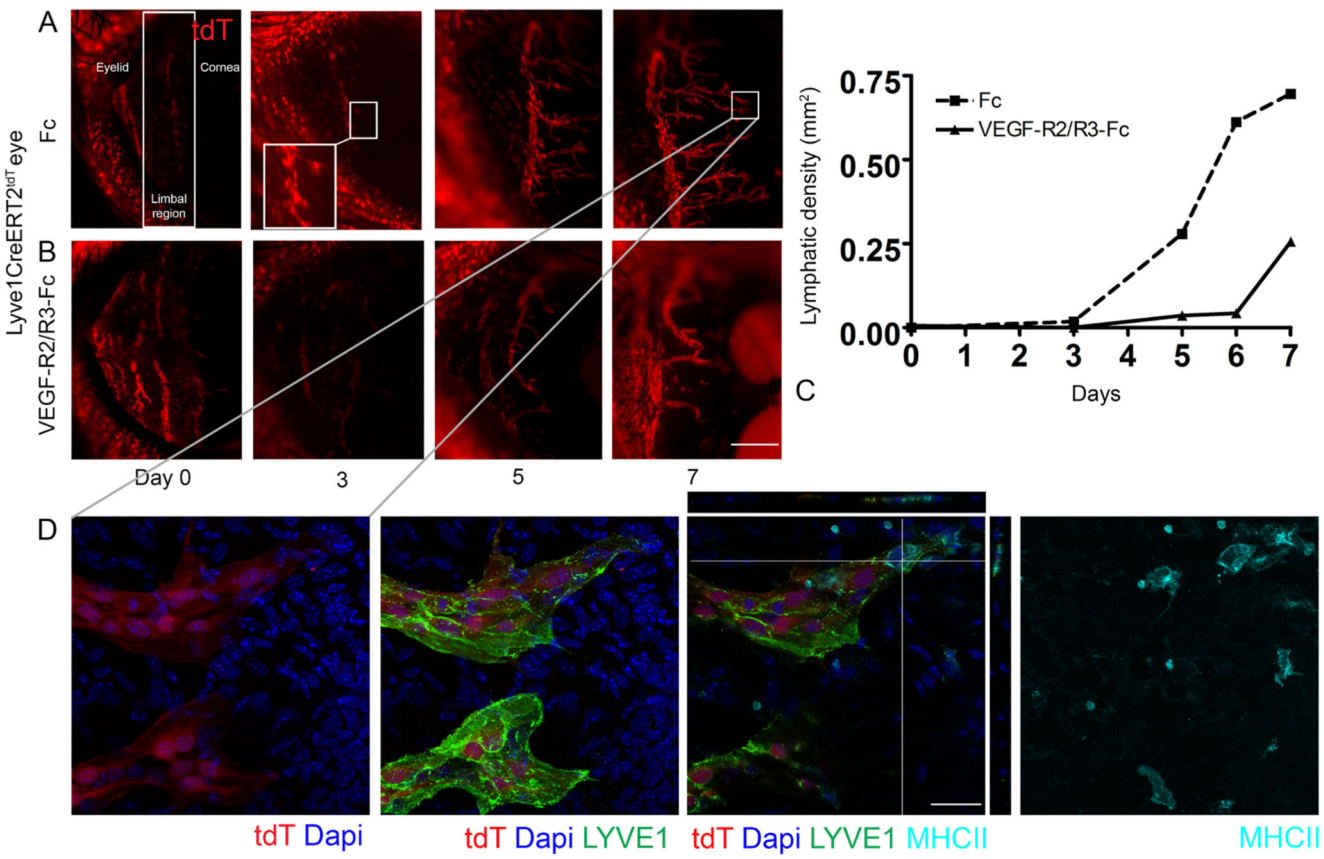

Figure 2.

Visualizing polyclonal tdT^{+} LECs expand during corneal lymphangiogenesis using live imaging. High dose 4-OHT was administered to Lyve1CreERT2^{tdT} mice, mice were rested 2 weeks, and corneal sutures were placed to stimulate lymphangiogenesis. The expansion of polyclonal tdT^{+} LEC precursors was visualized in individual Lyve1CreERT2^{tdT} mice treated with control Fc or VEGF-R2/R3 decoy receptors using live imaging fluorescent microscopy over the course of one week. New lymphatic vessel growth developed from the pre-existing limbal lymphatic vessel in Fc control conditions (Panel A). Administration of the VEGF-R2/R3-Fc decoy receptors inhibited tdT^{+} LEC proliferation and lymphangiogenesis (Panel B and C). High resolution MIP images obtained from confocal microscopy show endogenous tdT and Lyve-1 expression in LECs and MHC class II^{+} cells interfacing and possibly within tips of newly synthesized lymphatic vessels. Orthogonal views are shown (Panel D). This data are representative of 2 independent experiments with 3 mice in each group. The size standards are 500 μm in panel A and 100 μm in panel B.

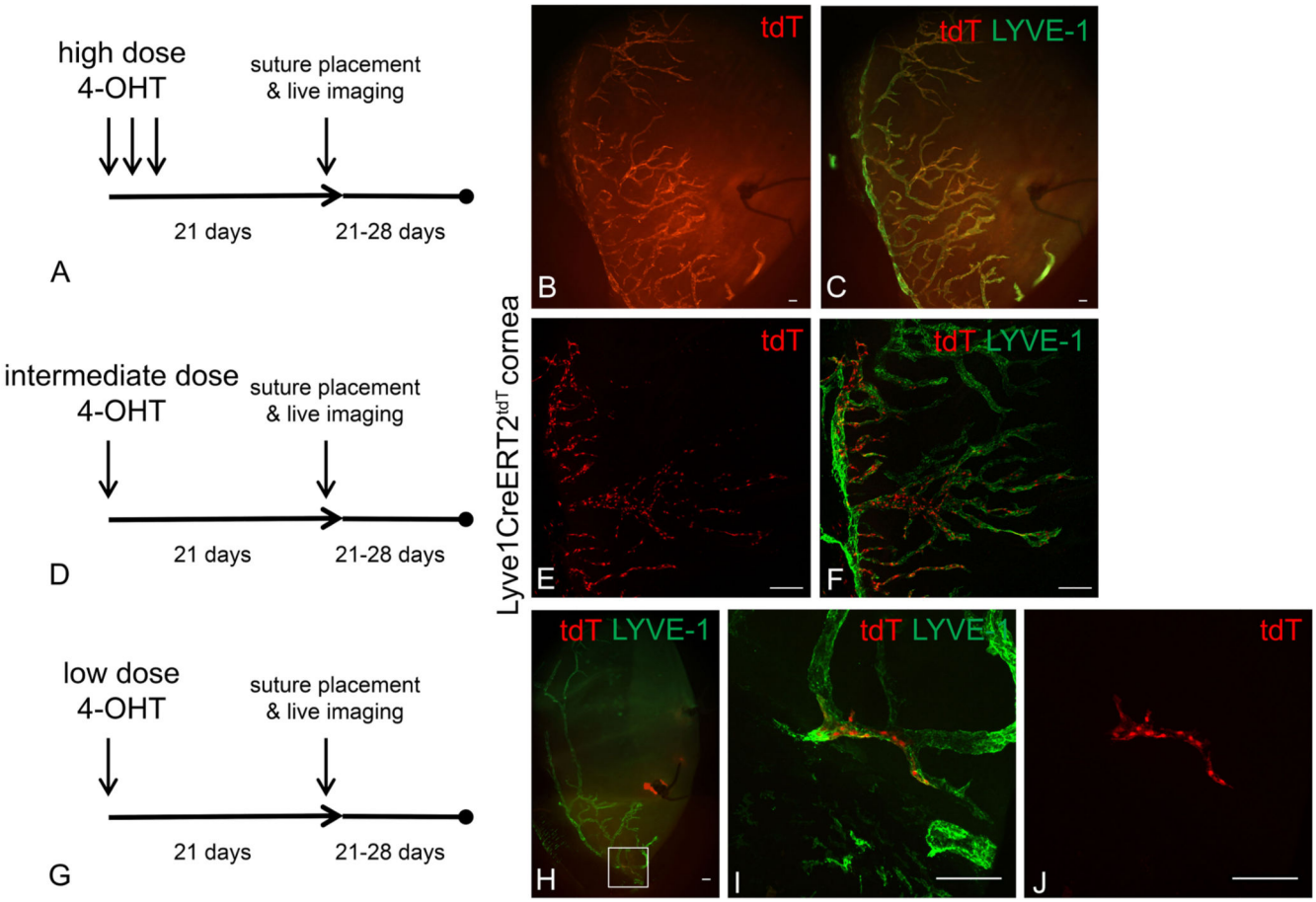

Figure 3.

Modifications to the 4-OHT dose and schedule produced a range of tdT expression patterns from nearly 100% to very few tdT^+ LYVE-1^+ LECS. Lyve1CreERT2^{tdT} mice were treated with high, intermediate, or low 4-OHT dosing schedules and rested for 3 weeks ensure the completion of tdT conversion and stability. Corneal lymphangiogenesis was stimulated using the suture induced model of corneal inflammation. Epifluorescence microscopy revealed that in high 4-OHT conditions, nearly all Lyve-1^+ LEC progenies were tdT^+ (A-C). In intermediate 4-OHT dose conditions, some of the Lyve-1^+ LEC progenies were tdT^+ shown by MIP confocal microscopy (D-F). In low 4-OHT dose conditions, very few of the Lyve-1^+ LEC progeny were tdT^+ shown by MIP confocal microscopy (G-J). In these conditions, LYVE-1^+ tdT^+ LEC progeny were distributed in a contiguous and relatively linear manner within a newly synthesized lymphatic vessel (J). This data are representative of 2 independent experiments with 3-4 mice per group. The image shown in J is representative of 6 LYVE-1^+ tdT^+ progenies visualized. The size standards are 100 μm.

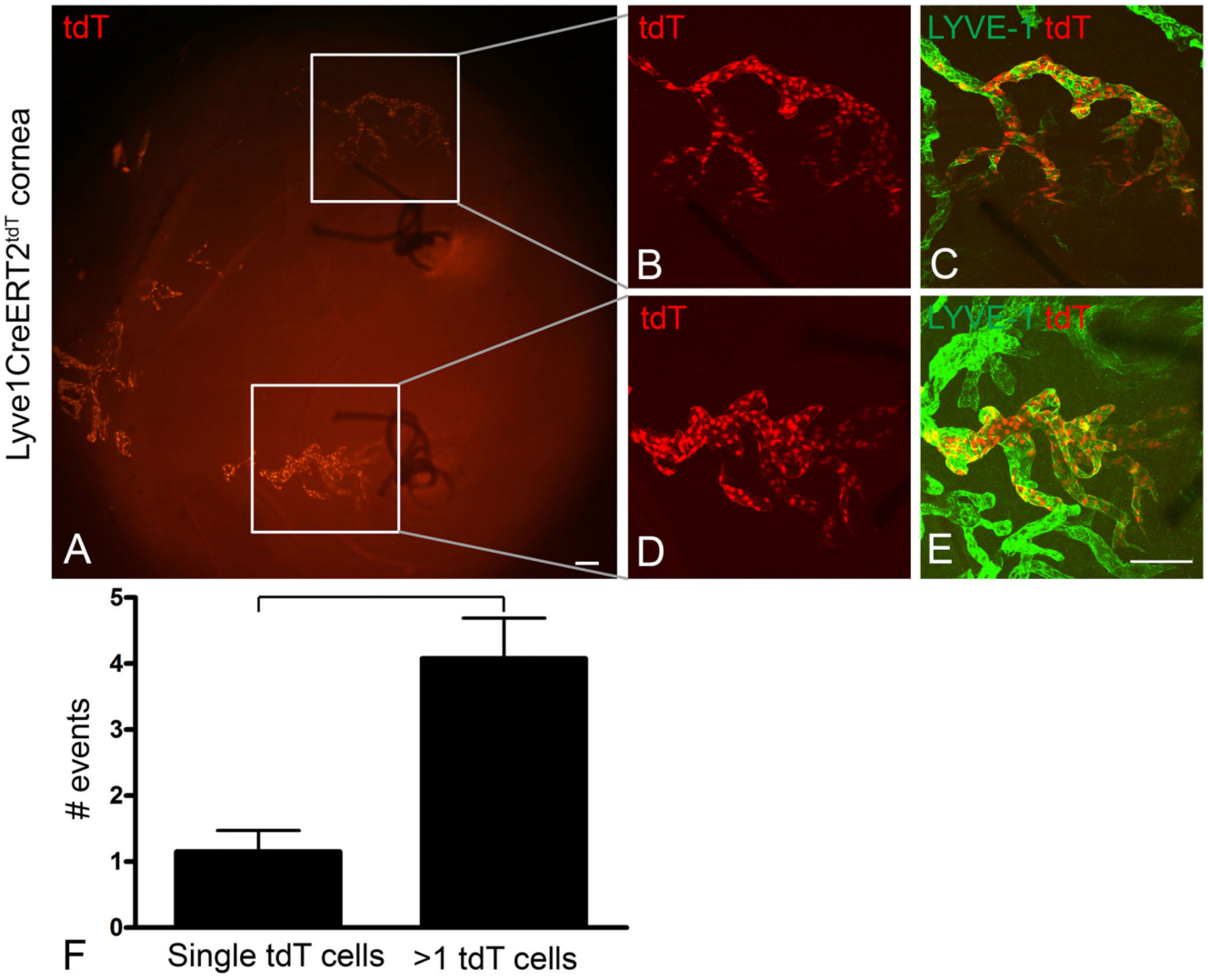

Figure 4.

Lymphatic endothelial lineage assemblage was identified in lymphatic vessels stimulated by suture induced inflammation for two weeks. Lyve1CreERT2^{tdT} mice were induced with intermediate doses of 4-OHT and rested for 3 weeks. Corneal lymphangiogenesis was stimulated using the suture induced model of corneal inflammation and the corneas were harvested after 2 weeks. Epifluorescence microscopy showed two sutures in the central cornea and the limbal region oriented to the left (A). LYVE-1 staining detected abundant lymphatic vessels, although this staining is not shown to highlight the presence of tdT^{+} LEC progenies assembled contiguously (A). Two representative LYVE-1^{+} tdT^{+} lineages visualized by high resolution MIP images obtained by confocal microscopy are shown in B, C and D, E. This data is representative of 2 independent experiments with 3 or 4 mice per experiment. An average of 1.2 single tdT^{+} LYVE-1^{+} LECs compared to an average of 4 groups of more than 1 tdt^{+} LYVE-1^{+} LECs were quantified in 7 individual Lyve1CreERT2tdT corneas (F). The difference in the number of these events was statistically significant. The size standards are 100 μm.

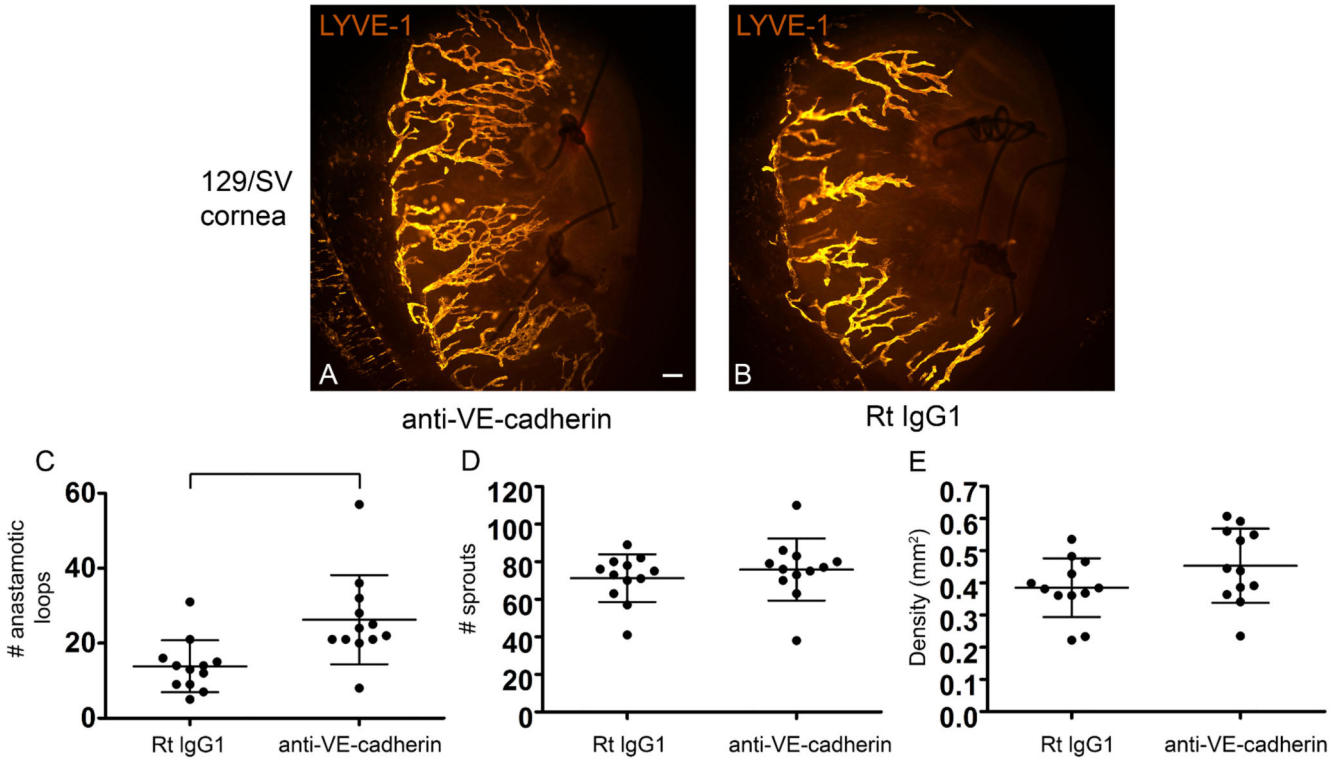

Figure 5.

VE-cadherin blockade induced increased lymphatic vessel loops within newly synthesized corneal lymphatic vessels *in vivo*. Suture induced corneal inflammation was used to stimulate new lymphatic vessel growth in 129/SV mice. Mice treated with neutralizing antibodies to VE-cadherin developed significantly more lymphatic vessel loop structures compared to isotype control treated mice (A-C). The lymphatic vessel density and sprout formation was similar between these groups (D and E). The data shown is from 3 independent experiments with 4 mice in each group, each dot representing a cornea. The bracket indicates a statistically significant difference. The size standards are 100 μm.

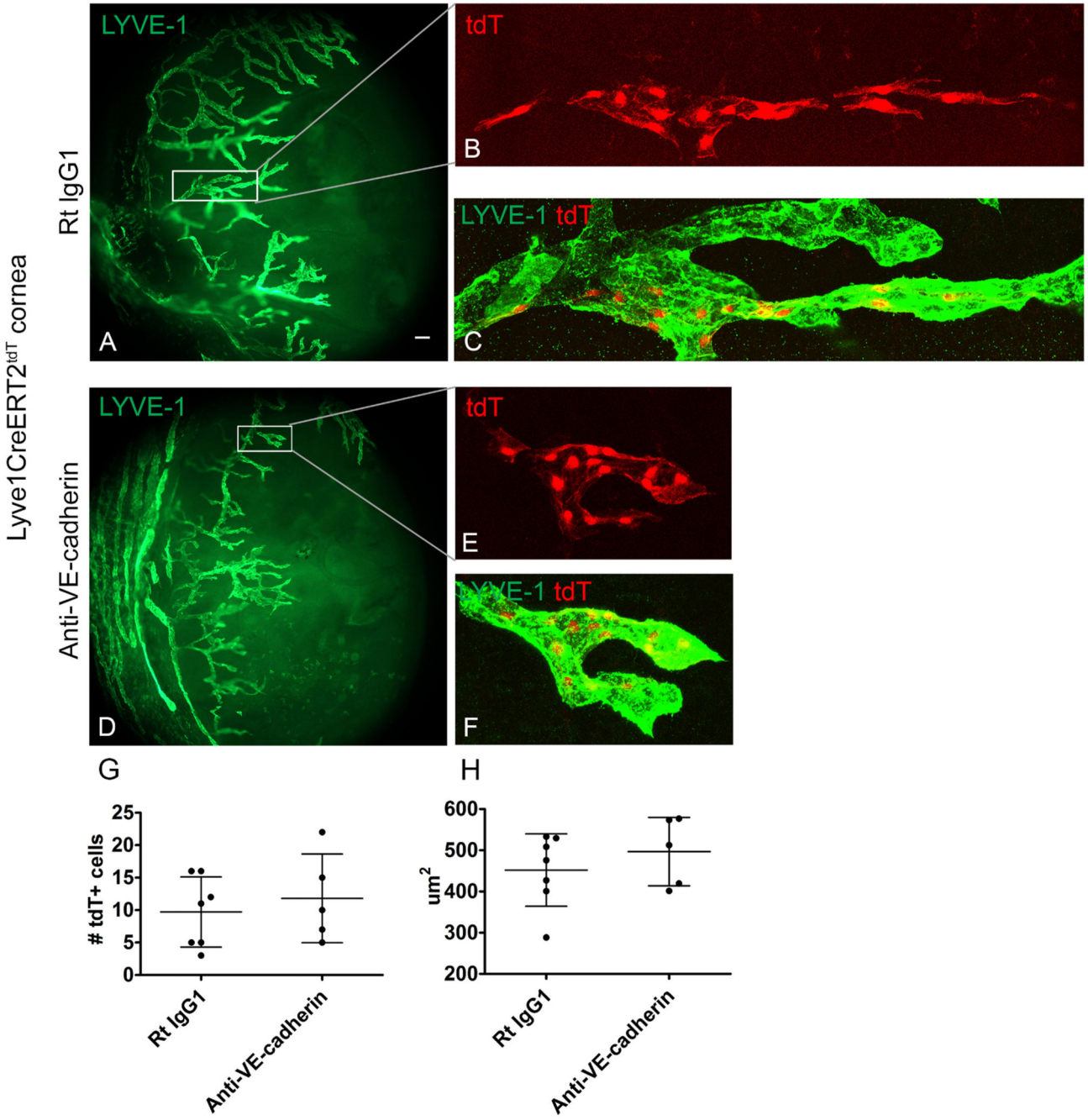

Figure 6.

VE cadherin blockade does not disrupt or potentate the contiguous assembly of newly synthesized LEC progeny. Low dose 4-OHT was administered to Lyve1CreERT2^{tdT} mice to induce tdT fluorescence expression in a low frequency of LECs. After 3 weeks, lymphangiogenesis was stimulated using the suture induced model of corneal inflammation. Groups of induced sutured Lyve1CreERT2^{tdT} mice were treated with isotype control or VE-cadherin blocking antibodies. Epifluorescent microscopy showed one or two groups of tdT^{+} LEC progeny per corneal hemisection, shown in inset (A). MIP obtained using confocal

microscopy showed contiguous arrangement of LYVE-1^+ tdT^+ LEC progeny in the Rat IgG1 isotype control conditions (inset in A shown in B and C). Contiguous tdT^+ LEC progeny were visualized in lymphatic vessels forming loops in Lyve1CreERT2^{tdT} mice treated with VE-cadherin blocking antibodies, inset in D is shown in E and F (D-F). In both conditions, groups of LYVE-1^+ tdT^+ LEC progeny were in direct cell to cell contact and had an average progeny size of about 10 cells (G). Individual tdT^+ LEC progeny in the Lyve1CreERT2^{tdT} mice treated with the VE-cadherin neutralizing or isotype control antibodies were similar in size (H). These results are pooled data from 12 progenies collected from 3 independent experiments with groups of 2-6 mice in each study. Some mice had no tdT^+ progenies. Size standards; for A and D are 100 μm and for B, C, E, and F are 50 μm.

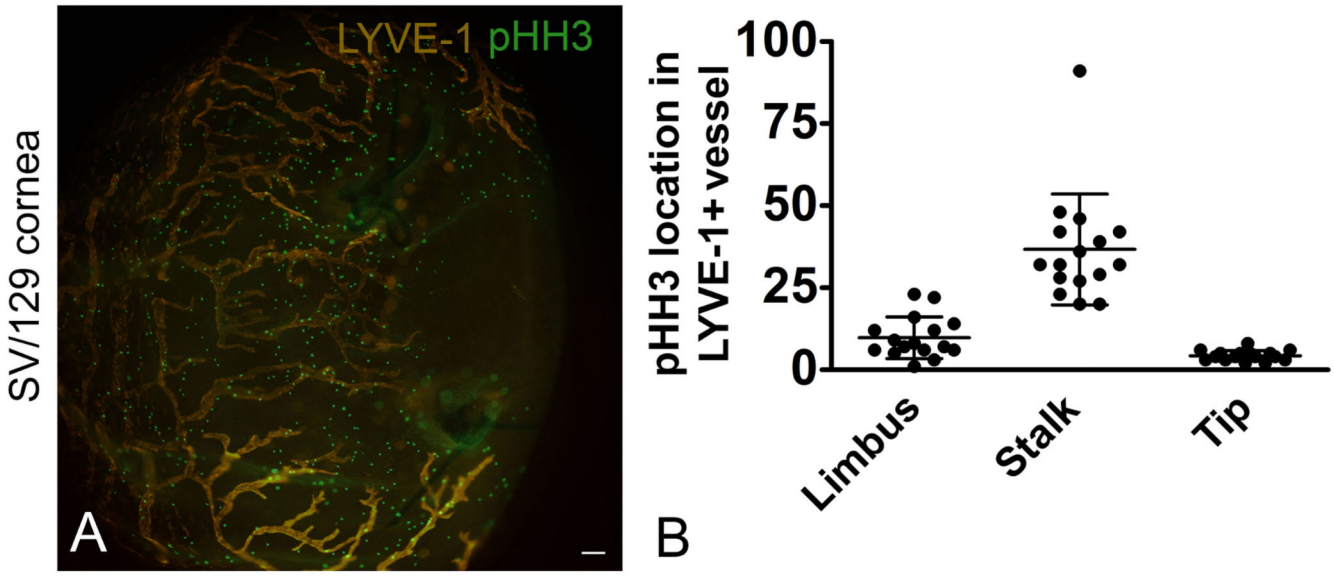

Figure 7.

Proliferating LEC stalk cells. Lymphangiogenesis was stimulated in SV-129 mice using the suture induced model of corneal inflammation. Corneas were labeled with antibodies to LYVE-1 and pHH3. An image obtained using epifluorescent microscopy is shown (A). Single z plane images were obtained using confocal microscopy from 14 individual mice. Random fields containing LYVE-1^{+} lymphatic vessels were identified and the localization of the pHH3 staining (limbus, stalk, tip) was quantified. pHH3 staining was the greatest in the LEC stalk cells (B). The data shown in B is composite data from 3 independent studies with 6 mice in each group, dots represents events per field. The size standard is 100 μM.

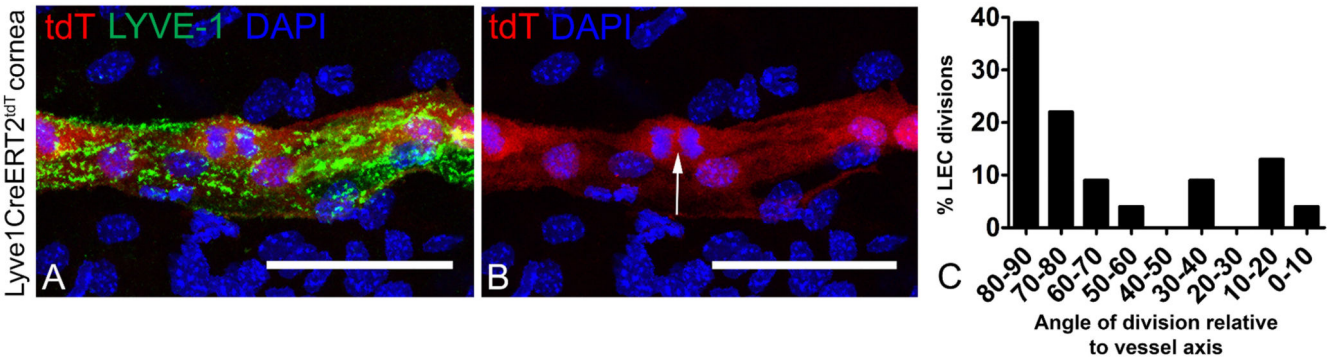

Figure 8.

High dose 4-OHT was administered to Lyve1CreERT2^{tdT} mice, the mice were rested for 2 weeks, and lymphangiogenesis was stimulated using the suture induced model of corneal inflammation. The mitotic plane relative to the long axis of the lymphatic vessel was measured in proliferating LYVE-1^{+} tdT^{+} LECs within newly synthesized corneal lymphatic vessels. Nearly all of these cells were in the stalk. Mitotic cells were identified by nuclear tdT and DAPI fluorescence patterns (A and B, arrow). The majority of the mitotic LECs had a mitotic plane 70-90 degrees relative to the long axis of the lymphatic vessel (C). Eleven random fields from 6 mice were scored and pooled results are shown (C, n=33). The size standards are 50 μm.

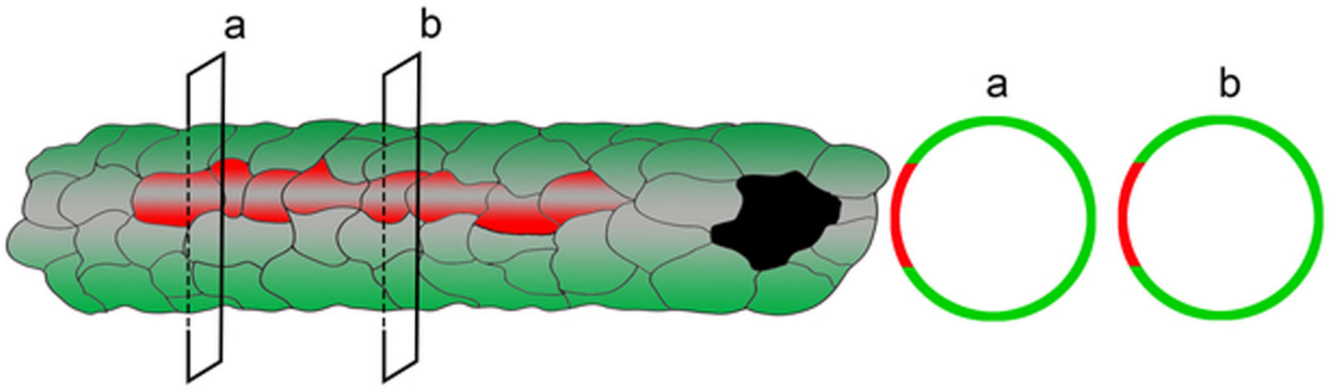

Figure 9.

Cartoon showing contiguously arranged tdT^{+} LEC progeny (red) assembled within a newly synthesized lymphatic vessel (green).